NJC

Accepted Manuscript

This is an *Accepted Manuscript*, which has been through the Royal Society of Chemistry peer review process and has been accepted for publication.

Accepted Manuscripts are published online shortly after acceptance, before technical editing, formatting and proof reading. Using this free service, authors can make their results available to the community, in citable form, before we publish the edited article. We will replace this *Accepted Manuscript* with the edited and formatted *Advance Article* as soon as it is available.

You can find more information about *Accepted Manuscripts* in the Information for Authors.

Please note that technical editing may introduce minor changes to the text and/or graphics, which may alter content. The journal's standard Terms & Conditions and the Ethical guidelines still apply. In no event shall the Royal Society of Chemistry be held responsible for any errors or omissions in this *Accepted Manuscript* or any consequences arising from the use of any information it contains.

ROYAL SOCIETY OF CHEMISTRY

www.rsc.org/njc

NJC

PERSPECTIVE

A design concept of amphiphilic molecules for directing hierarchical porous zeolite

Received 00th /// 20xx,
Accepted 00th /// 20xx

DOI: 10.1039/x0xx00000x

www.rsc.org/

Dongdong Xu[a], Shunai Che[b,*] and Osamu Terasaki[c]

Aluminosilicate zeolites with hierarchically porous system have attracted special scientific interest due to their advantages in bulky molecule catalysis. Organic amphiphilic molecules or surfactants are frequently employed into the hydrothermal synthesis of porous zeolite for the construction of enhanced pore system (mesopores or macropores) beyond the sole micropores. This review describes a design concept of novel amphiphilic molecules for one-step preparation of hierarchically porous zeolites containing mesopores with certain orders. Via the structural-directing mechanism study of the most common surfactant (cetyltrimethyl ammonium bromide, CTAB) in the synthesis of bulk zeolite MFI (zeolite framework code by International Zeolite Association), aromatic groups were reasoningly grafted in the hydrophobic tail of the amphphilic molecule. Due to the π-π stacking of aromatic groups and a geometrical matching between their arrangement and the zeolitic framework, single-crystalline zeolite nanosheets (SCZN) were successfully synthesized. Furthermore, following the same idea for design, bolaform and triply branched amphiphilic molecules with aromatic groups were also prepared and used for the formation of SCZN with 90° rotational boundary and single-crystalline mesoporous ZSM-5 with three-dimensional pores, respectively. This design concept will provide a new insight into the molecular factors for governing the simultaneously fabrication of ordered meso- and micro-phases.

1. Introduction

Zeolites, as a kind of highly efficient crystalline catalysts, have brought about great economic benefits, especially in the field of petrochemical industry[1-5]. However, when considering that the pore size of zeolite generally goes below 1 nm, it would greatly restrict their catalytic performance involving organic molecules with lager dimension[6-8]. For purpose of the accommodation between micropore size and organic molecular dimension, many researchers have made great efforts to build zeolitic frameworks with larger aperture or introduce another set of pore system (mesopores or macropores) into the bulk zeolite crystals[9-11]. In the past two decades, along with the development of hydrothermal synthesis and mechanism study of ordered mesoporous silica[12-15], many innovative techniques were used to prepare zeolites with hierarchically porous system.

So far, a lot of reports have focused on the fabrication of hierarchically porous zeolites[11, 16-19]. The methods can be categorised into four: i) stack and assembly of zeolitic microcrystals, ii) the removal of framework atoms (or post-synthetic modification), iii) hard-templating method, iv) soft-templating strategy[20-22]. When some small zeolite crystals (or seeds) stack together, there are plenty of gap between them which is generally called intercrystalline pores[23-27]. Based on the characteristic crystal growth of some kinds of zeolites, intracrystalline pores are created, such as silicalite-1 with 90° rotational intergrowth[28], self-pillared pentasil zeolite with house-of-cards-like morphology[29, 30]. Generally, it is not easy to control pores in size and arrangement. The selective removal of silicon (desilication) or aluminium (dealumnization) from the zeolite framework can more or less produce some mesopores[31-33]. A lot of work in the area of desilication has been tried to build porous zeolites, for example by Pérez-Ramírez and co-workers[34-36]. Any removable inert species can be applied as the hard templates to create mesopores inside bulk zeolites, for example, carbon nanoparticles[37], nanowires[38], nanotubes[39], aerogel[40], ordered

*"**An exciting journey in the creative word of ordered porous materials and their applications**" dedicated to Francois Faujula on the occasion of his retirement.*

[a] *Jiangsu Key Laboratory of Biofunctional Materials, School of Chemistry and Materials Science, Nanjing Normal University, Nanjing, 210023, P. R. China*
[b] *School of Chemistry and Chemical Engineering, State Key Laboratory of Metal Matrix Composites, Shanghai Jiao Tong University, 800 Dongchuan Road, Shanghai, 200240, China. Corresponding Author, E-mail: chesa@sjtu.edu.cn*
[c] *Department of Materials & Environmental Chemistry. Stockholm University, Stockholm, Sweden.*

Dongdong Xu graduated from Nankai University, P. R. China, in 2009 with a B.Sc. in Chemistry, and received his Ph.D. from Shanghai Jiao Tong University in 2014, under the supervision of Prof. *Shunai Che*. He is currently a Lecturer in the School of Chemistry and Materials Science at Nanjing Normal University, P. R. China. His research interests mainly focus on the construction of inorganic metal porous architecture based on the self-assembly of surfactants.

Shunai Che is a Professor in the Departmen Chemistry, School of Chemistry and Chemical Engineering, Shanghai Jiao Tong University. She was born in 1964 and received her Ph.D. degree from the Yokohama National University. She was a guest researcher at Saitama University and worked as a postdoctoral fellow at the Yokohama National University. She moved to her current position in January 2004. Her research interests encompass the development of chiral inorganic materials and porous materials with novel structures and functions, in view of applications in optical devices and heterogeneous catalysis.

Osamu Terasaki was a faculty member for 35 years in the Dept of Physics, Tohoku Univ, Japan. He moved and became the head of Structural Chem, Stockholm Univ (SU), Sweden in 2003. After retirement from the head, he is currently Profs Stockholm Univ and BK21+ KAIST, Korea, a Visiting Prof UC Berkeley and a Distinguished Adjunct Prof Shanghai Tech. He has received the Friendship Award from P.R. China (2003), the Donald W. Breck Award from the Int Zeolite Association (2007) and the Humboldt-Research Award from the Alexander von Humboldt Foundation (2008). His interest lies in developing scattering/diffraction/imaging approaches suitable for understanding characteristic features of nanostructured materials from structural aspects.

mesoporous carbon[41, 42], organic sponge and foam[43], $CaCO_3$ nanoparticles[44]. In order to produce ordered mesopores inside zeolites, 3-dimensinonal ordered mesoporous carbon with larger mesopores developed by Tsapatsis and co-workers is employed into the hydrothermal synthesis of ordered porous zeolites (like mesoporous MFI, LTA, FAU, BEA)[45, 46]. Most of zeolites with mesopores in their crystals (hereafter mesoporous zeolites) obtained by the above methods have shown fine catalysis performance as was expected.

Soft-templating strategy mainly depends on the self-assembly of amphiphilic molecules and is most feasible to fabricate ordered mesopores and micropores simultaneously[47-51]. Amphiphilic organosilanes, in which the silicon part was linked to the terminal close to quaternary ammonium, can serve as mesoscale templates and effectively adhere to the zeolite crystal faces to further form well mesostructure[52-56]. For example, 3-(trimethoxysilyl) propyl-hexadecyldimethylammonium chloride and the analogues with different chain lengths were firstly used by Ryoo *et al* to prepare mesoporous zeolites. Mesoporous MFI zeolites with tunable mesopore diameters were obtained after calcination to remove the organic templates[52]. When amphiphilic organosilanes were added into the synthesis precursor of FAU-type zeolite[57], mesoporous zeolite X with a threefold hierarchical pore system, which was constructed of zeolitic nanosheets in a house-of-cards-like assembly with plenty of interstices between the nanosheet stacks, was prepared. Pinnavaia *et al* reported a method to prepare zeolites with small intracrystal mesopores by using a silane-functionalized polymer which could be treated as a kind of special amphiphilic organosilanes[56]. Xiao *et al* developed the hydrophilic cationic polymer to produce abundant mesopores inside zeolites[58-60]. Single-crystalline mesoporous zeolite Beta and ZSM-5 were obtained with polydiallyldimethylammonium chloride (PDDA) and polystyrene-*co*-4-polyvinylpyridine, respectively[61, 62]. However, all of these cases mentioned above, the mesoporous structure are still disordered.

In order to introduce ordered mesopores into zeolites, Ryoo and co-workers have successfully prepared a series of amphiphilic molecules with double or multiple quaternary ammoniums[63]. These bifunctional surfactants, as the effective structural-directing agents (SDAs), could direct the formation of zeolitic framework and a mesoscale micellar structure, simultaneously. Diquaternary ammonium surfactant, represented by $C_{22}H_{45}$-$N^+(CH_3)_2$-C_6H_{12}-$N^+(CH_3)_2$-C_6H_{13} ($2Br^-$), was successfully utilized as a sole SDA to synthesize the MFI zeolite nanosheets with a single-unit-cell thickness along *b*-crystallographic axis[64-71]. Furthermore, a tri-quaternary ammonium surfactant with the chemical formula of $C_{18}H_{37}$-$N^+(CH_3)_2$-C_6H_{12}-$N^+(CH_3)_2$-C_6H_{12}-$N^+(CH_3)_2$-$C_{18}H_{37}$ ($3Br^-$) could produce a hexagonally-ordered mesoporous material where the silica walls consisted of a truly crystalline zeolitic framework[72, 73].

Table 1 Summary of the construction of hierarchically porous zeolites by using various soft-templating strategies.

Soft-templating strategy	Templates	Mesoporous structure	Type of zeolitic framework	Ref.
Double templating (large organic templates + small SDAs)	Cationic surfactants (e. g. CTAB)	Tunable but disordered mesoporosity	ZSM-5, Beta, Y	47-49
	Anionic surfactants		NaA	50
	Amphiphilic organosilane		MFI, FAU, BEA	52-55
	Silylated polymer		ZSM-5	56, 57
	Cationic polymers (e.g. PDDA)		BEA, ZSM-5, X	58-60, 62
	Non-ionic polymers (e. g. P_{123}, F_{127}, PVB)		MFI, LTA, BEA	51
Bifunctional amphiphilic molecules	Diquaternary ammonium surfactants	Lamellar nanosheets	MFI, MTW	64-71
	Polyquaternary ammonium surfactants	Hexagonal mesopores	Zeolite-like, BEA	72-73
	Multiamines surfactants	Lamellar nanosheets	AEL, AFI, ATO	75
	Cationic polymers	Disordered	BEA, MFI	61, 74
	Single quaternary ammonium surfactants	Lamellar nanosheets	MFI	79-80

This type of templates can also be used to fabricate microporous aluminophosphate nanosheets and their analogues, such as silicoaluminophosphate, cobalt aluminophosphate, and gallium phosphate[74, 75]. The above synthesis strategy allows for the fine control of both zeolitic framework type and micellar structure by single organic template. The various strategies for the construction of hierarchically porous zeolites by soft-templating are summarized in Table 1.

Although many kinds of mesoporous zeolites have been successfully synthesized so far, how to understand the cooperative formation mechanism between ordered meso-phase and micro-phase structures and construct more variety of hierarchically porous zeolites with diverse topological framework remains a big challenge[76, 77]. In our works, we aimed to make clear the structural-directing mechanism of different amphiphilic molecules beginning with familiar CTAB and further designed novel amphiphilic molecules to prepare ordered mesoporous zeolites. Figure 1 shows the design process of our strategy for novel amphiphilic molecules and the molecular configuration toward to the synthesis of ordered mesoporous zeolite. Firstly, the structural-directing mechanism of CTAB in the synthesis of bulk zeolite MFI was studied in detail, indicating that the quaternary ammonium head groups can serve as SDAs for zeolites, and the long chains become isolated and occupy the micropores[78]. Secondly, through the introduction of aromatic groups into the hydrophobic chain (Fig. 1b), the π-π stacking coming from benzene rings could effectively limit the crystal growth along *b*-crystallographic axis of the MFI framework and direct the formation of lamellar single crystalline mesostructured zeolite nanosheets (SCZN)[79, 80]. Thirdly, based on the computer simulation using molecular mechanics calculations, it indicated that the coexistence of diquaternary ammonium head and aromatic groups would significantly reduce the total binding energies of mesostructured zeolite synthesis system[80]. Therefore, we designed a kind of bolaform amphiphilic molecules (Fig. 1c) and SCZN with 90° rotational boundaries was synthesized. Furthermore, in order to restrict the sole crystal growth along *a*- or *c*-axis, we introduced another branch in the bolaform molecules which was called triply branched cationic surfactant (Fig. 1d). When this molecule was used in the hydrothermal synthesis system of zeolite MFI, single-crystalline mesoporous ZSM-5 (SCMZ) with three-dimensional pores was successfully obtained[81]. Along with the evolution of molecular configuration (Fig. 1a-d), it realized the construction of hierarchically mesoporous zeolites from bulk to two-dimensional and three-dimensional[78-81]. Our strategy for designing the amphiphilic molecules mainly focuses on the interactions between the hydrophobic carbon chains, which is different from previous pathways mentioned above. It opens up a new approach for the molecular design and the subsequent preparation of porous zeolites. Additionally, the obtained materials by our strategy possess unique both mesoporous and microporous structure which will be showed in the following statement.

2. Structural-directing mechanism of CTAB

As is well known, the role of conventional quaternary ammonium salts in the formation of zeolites generally attributes into three categories: i) space-filling species, ii) structural directing agents, and iii) templates[82-87]. However, when cationic surfactants with long alkyl chain (e.g. CTAB) were tried to synthesize zeolites, amorphous mesoporous silica instead of crystalline zeolites were obtained without decomposition of these surfactants at high temperatures[86-90]. In order to understand the role of cationic surfactants in the construction of micropores and further lay a foundation for the design of novel amphiphilic molecules to produce mesoporous zeolites, we attempted to synthesize zeolites using CTAB as the sole template through the fine adjustment of the synthesis conditions[78].

Via the comparison of synthesis results under different temperatures, it indicated that 150 °C was most appropriate for CTAB to direct the formation of ZSM-5 without any decomposition which could be visually confirmed from the Scanning Electron Microscope (SEM) image in Figure 2. The particular synthesis composition, such as CTAB concentration and the SiO_2/Al_2O_3 molar ratio, was well investigated at 150 °C. Under appropriate original

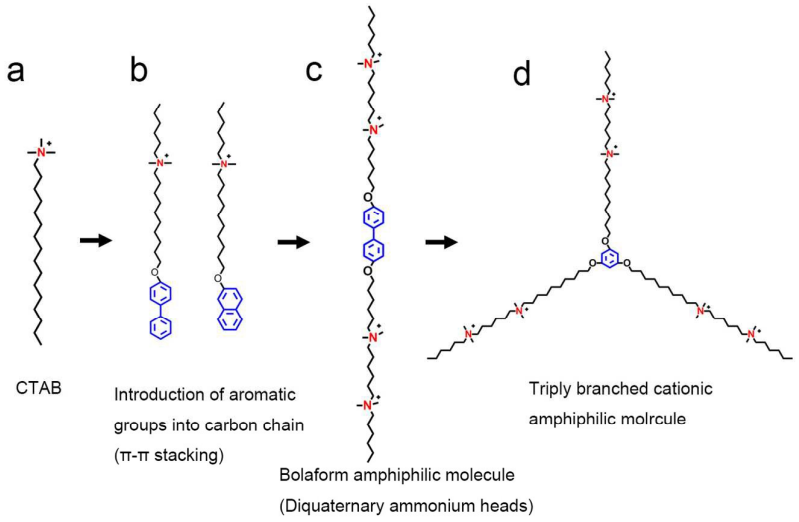

Fig. 1 The design thought of novel amphiphilic molecules and the corresponding molecular configuration.

composition, pure zeolite MFI (ZSM-5 or silicalite-1) with high crystallinity were successfully obtained. That is, CTAB can really direct the formation of zeolites. With the purpose of exploring the existence of the surfactant CTAB in the micropores, a ZSM-5 sample prepared under the molar composition of CTAB: SiO_2 : Al_2O_3 : Na_2O : H_2O = 1 : 20 : 0.2 : 2.5 : 800 at 150 °C was employed for the detailed characterization of IR spectra, ^{13}C NMR spectra , thermal-gravity and elemental analysis. Based on the above characterization results, it indicates that the CTAB surfactant indeed acts as a SDA without any decomposition and only half of the total micropores in MFI frameworks are occupied by the ammonium groups while other species are present in the other half.

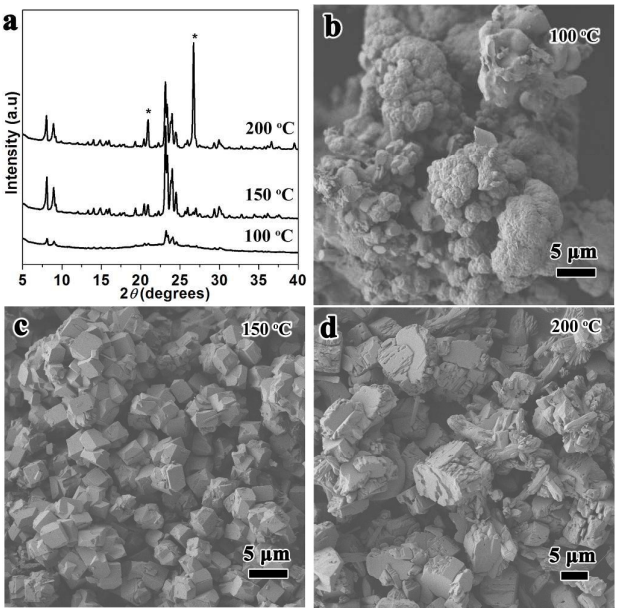

Fig. 2 The XRD patterns (**a**) and the SEM images of the zeolite products synthesized at different temperatures of 100 (**b**), 150 (**c**) and 200 °C (**d**). Reprinted with permission from ref. 78. Copyright 2014. Royal Society of Chemistry.

As a consequence, the most possible structural-directing mechanism of CTAB is proposed as shown in Fig. 3. A single CTAB molecule participates in the formation of two micropores. The ammonium head acts as the SDA, and the hydrophobic tail plays the space-filling role. This kind of model for the location of CTAB molecules in the channels of the MFI zeolite is also recommended by Okubo and co-workers almost at the same time[91]. All of the results demonstrate that cationic surfactants with long hydrophobic alkyl chain can play a role of SDA for the formation of zeolites but undergo the distinct mechanism. It provides new insights for the various surfactants commonly used in the synthesis of mesoporous materials to direct the construction of zeolites and the ones with hierarchically porous system.

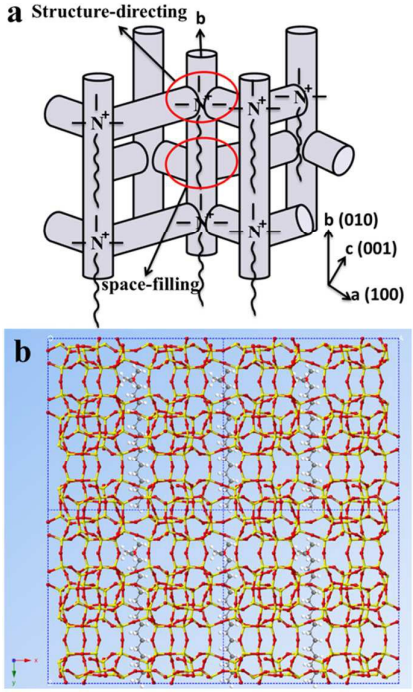

Fig. 3 Schematic illustration of the role of CTAB in the structural-directing formation of MFI zeolite. Reprinted with permission from ref. 78. Copyright 2014. Royal Society of Chemistry.

3. Single-crystalline mesostructured zeolite nanosheets owing to the π-π stacking

Although CTAB can direct the formation of zeolite MFI and the hydrophobic chains are located in the straight channel of MFI framework, the sole hydrophobic interactions between the alkyl chains cannot prevent the crystal growth along *b*-axis. In view of this point, we deduced that the interactions between hydrophobic tails would be greatly enhanced and therefore could effectively block the crystal growth if certain specific groups could be connected in the carbon chain. Finally, zeolites with ordered mesopores will most possibly be obtained. The π-π stacking interaction is a kind of common non-covalent intermolecular forces and is widespread in biological and chemical system from molecular recognition to self-assembly[92-96]. As a consequence, we designed a series of amphiphilic molecules functionalized by connecting aromatic groups (such as biphenyl and naphthyl) to the terminal of carbon chain (Fig. 1b)[80]. When these templates are used as a sole organic agent to synthesize zeolite, single crystalline lamellar mesostructured zeolite nanosheets (denoted as SCZN-1) were successfully generated under certain hydrothermal synthesis conditions. Figure 4 shows the structural characterization of SCZN-1 synthesized by C_6H_5-C_6H_4-O-$C_{10}H_{20}$-$N^+(CH_3)_2$-C_6H_{13} (Br^-) (denoted as $C_{Ph-Ph-10-6}$). X-ray diffraction (XRD) pattern (Figs. 4a-b) of SCZN-1 indicated the formation of layered MFI nanosheets with new unit cell (4.8 nm) and SEM image (Fig. 4c) showed uniform morphology, corresponding to the observation from high-resolution transmission electron microscopy (HRTEM).

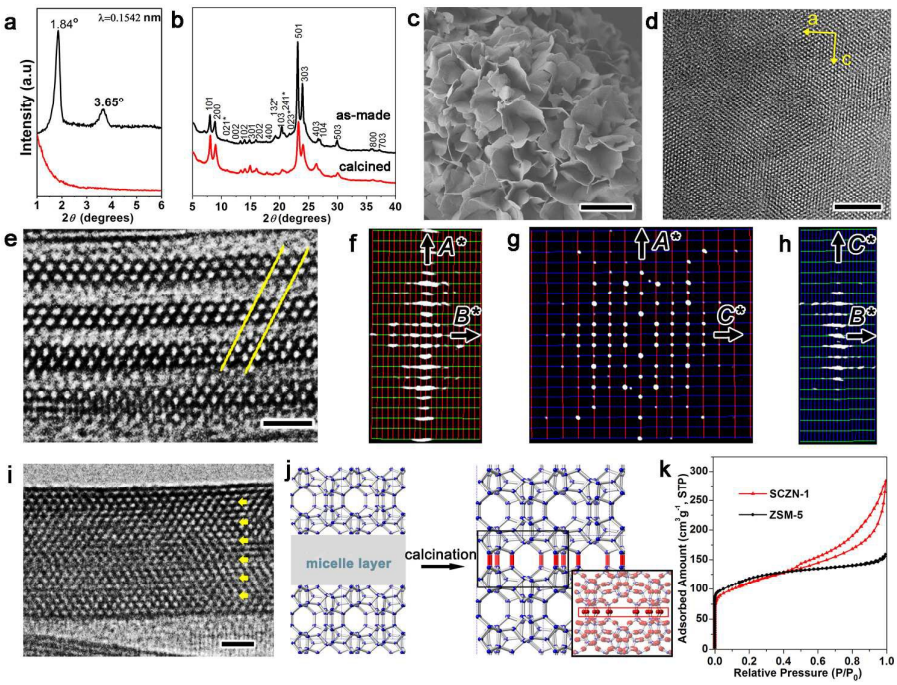

Fig. 4 Structural characterization of SCZN-1. (a, b)XRD patterns, (c) SEM image, (d, e) HRTEM of the as-made SCZN-1. (f–h) 3D EDT projections with multiple unit cell meshes along different directions. (i) HRTEM image taken along the [100] axis of the calcined sample. (j) Structural model of SCZN-1 before and after calcination. (k) The N2 adsorption-desorption isotherms of calcined SCZN-1 and conventional ZSM-5. The scale bars in c, d, e and i represent 2 μm, 20 nm, 5 nm and 5 nm, respectively. Reprinted with permission from ref. 80. Copyright 2014. Nature Publishing Group.

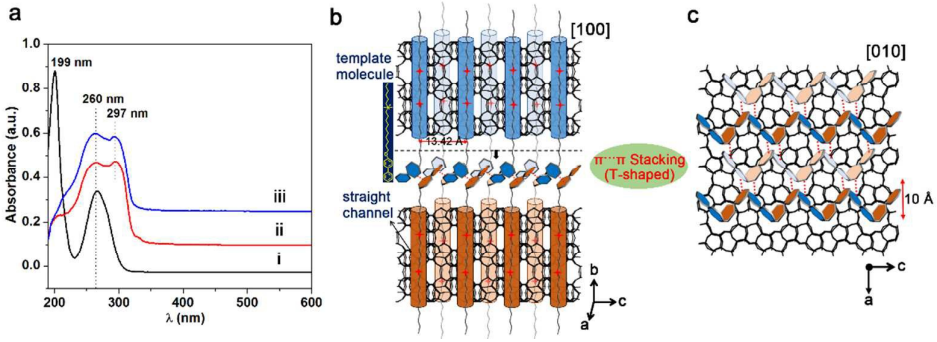

Fig. 5 Schematic representation of π-π stacking in SCZN-1. (a) UV-visible absorption spectra of template molecules in a dilute water solution (i), in the crystalline solid (ii) and in the as-made SCZN-1 (iii). (b, c) The arrangement model of biphenyl groups observed from the straight channel and a-c plane, respectively. Reprinted with permission from ref. 80. Copyright 2014. Nature Publishing Group.

Interestingly, SCZN-1 possesses the single-crystalline mesostructure which could be directly observed from HRTEM images (Fig. 4d-e). Three-dimensional electron diffraction tomography (3D EDT) data revealed the high structural coherence of the MFI sheets[97]. The super lattice arising from registered MFI layers was determined to be rhombic with new cell parameters of a = 20.5 Å, b = 40.3 Å and c = 13.9 Å (Figs 4f-h). Owning to the single-crystalline property, crystallographically ordered MFI sheets could connect with each other to single crystals via the formation of new Si-O-Si bonds after calcination (Figs. 4i-j).

The presence of π-π stacking can be confirmed via UV-Vis absorption spectroscopy with a red shift of the absorption band at 297 nm (Fig. 5a). Additionally, the position of the aromatic rings (in the middle of micelle) was verified via electron charge distributions based on low-angle XRD data. Combining with ^{13}C NMR spectra, elemental analysis and TEM observation, the arrangement of aromatic groups in the as-made SCZN-1 was speculated as shown in Figs. 5b and c. The ammonium groups of the amphiphilic molecules are located in the straight channel of MFI framework to direct the formation of MFI micropores and the aromatic groups in the hydrophobic tails to generate stable network with strong π-π

stacking. All of the biphenyl groups possess a T-shaped configuration with a well-defined network, which geometrically matches the MFI frameworks and produce the single-crystalline MFI layers.

The necessity of π-π stacking for the construction of single-crystalline MFI layers is further identified via changing the length of carbon chain between biphenyl group and quaternary ammonium head and the number of benzene ring[79]. From powder XRD patterns (Fig. 6) and SEM images (Fig. 7) of as-made zeolites synthesized by using different surfactants, it indicates that the presence of one benzene ring or a short carbon chain in the hydrophobic part cannot empower the surfactants with a single quaternary ammonium head group to direct SCZN except for bulk ZSM-5. A lamellar mesostructure is obtained only when the alkyl group in the surfactants was varied above C6 where the effective and strong π-π stacking turns up.

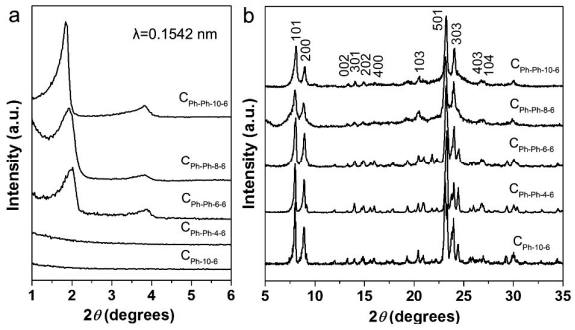

Fig. 6 Low-angle (a) and high-angle (b) powder XRD patterns of as-made zeolites synthesized by different single-head ammonium surfactants. Reprinted with permission from ref. 79. Copyright 2014. American Chemical Society.

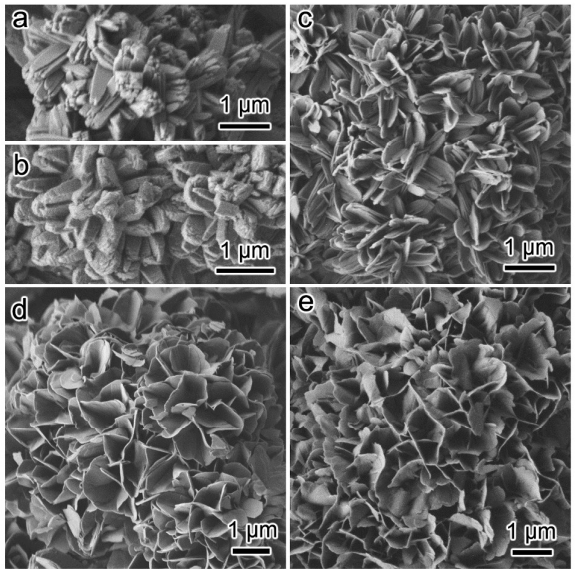

Fig. 7 SEM images (a-e) of as-made zeolites synthesized by the surfactants $C_{Ph\text{-}10\text{-}6}$ (a), $C_{Ph\text{-}Ph\text{-}4\text{-}6}$ (b), $C_{Ph\text{-}Ph\text{-}6\text{-}6}$ (c), $C_{Ph\text{-}Ph\text{-}8\text{-}6}$ (d), $C_{Ph\text{-}Ph\text{-}10\text{-}6}$ (e). Reprinted with permission from ref. 79. Copyright 2014. American Chemical Society.

In order to understand why the single-head quaternary ammonium amphiphilic molecules containing aromatic groups ($C_{Ph\text{-}Ph\text{-}10\text{-}6}$) could form lamellar-structured MFI nanosheets, molecular mechanics calculations were applied to compare the relative stabilities of bulk and layered MFI zeolite structures with different template molecules[98, 99]: $C_{Ph\text{-}Ph\text{-}10\text{-}6}$, single-head $C_{22}H_{45}N^+(CH_3)_2C_6H_{13}$ ($C_{22\text{-}6}$) and diquaternary ammonium type template $C_{22}H_{45}N^+(CH_3)_2C_6H_{12}N^+(CH_3)_2C_6H_{13}$ ($C_{22\text{-}6\text{-}6}$). The calculation results indicate that the layered structure is more stable than the bulk one in $C_{Ph\text{-}Ph\text{-}10\text{-}6}$ and $C_{22\text{-}6\text{-}6}$ system (Table 2). The presence of both the second quaternary ammonium head and the biphenyl groups would greatly reduce the binding energies of the zeolitic synthesis system. However, a thorough analysis of the calculated energies reveals that the stabilizations depend on different mechanisms. For $C_{22\text{-}6\text{-}6}$, the electrostatic interactions between the quaternary ammonium groups outside of the MFI slabs and the slab surfaces contribute the most to the binding energy. As for $C_{Ph\text{-}Ph\text{-}10\text{-}6}$. The π-π interactions among the biphenyl groups play a key role to stabilize the MFI nanosheet model.

Table 2 Different calculated binding energy in the three amphiphilic molecules-MFI systems. Reprinted with permission from ref. 80. Copyright 2014. Nature Publishing Group.

Templates	E_b (kJ · mol^{-1})		ΔE_b (nanosheet-bulk)
	Bulk	nanosheet	kJ·mol^{-1}
$C_{22\text{-}6}$	-104.5	-93.6	10.9
$C_{22\text{-}6\text{-}6}$	-114.0	-152.2	-38.2
$C_{Ph\text{-}Ph\text{-}10\text{-}6}$	-439.6	-487.1	-47.5

4. Bolaform amphiphilic molecules directing for 90° rotational intergrowth structure

As related above, the periodic interlamellar structural order in SCZN-1 will disappear after the removal of organic templates. How to remain the mesoporous structure is still a big challenge. It is well known that MFI zeolite is often formed with 90° rotational intergrowths, in which substantial (*h*00) faces are epitaxially overgrown on the (0*k*0) faces[100-103]. Through engineering the zeolite intergrowths, hierarchically organized structure can be constructed owning to the framework connectivity even after calcination. However, this kind of special structure always entails high binding energies. Based on our calculation results, the coexistence of diquaternary ammonium head and biphenyl groups would greatly reduce the total binding energies of zeolite synthesis system. Therefore, we connected these two groups into single organic molecule as the form of bolaform amphiphilic molecules C_6H_{13}-$N^+(CH_3)_2$-$(CH_2)_6$-$N^+(CH_3)_2$-$(CH_2)_n$-O-C_6H_4-C_6H_4-O-$(CH_2)_n$-$N^+(CH_3)_2$-$(CH_2)_6$-$N^+(CH_3)_2$-C_6H_{13} ($4Br^-$) (denoted as $BC_{Ph\text{-}n\text{-}6\text{-}6}$). Single-crystalline zeolite nanosheets with 90° rotational boundaries (SCZN-2) are successfully synthesized using these bolaform molecules under certain hydrothermal synthesis gel[80].

As shown in Fig. 8, the SEM images revealed that all of these SCZN-2 obtained by using bolaform molecules with different carbon chain have an extraordinary boundary structure with the 90° rotation of adjacent faces. Interestingly, it was found that the number of 90° rotational crystals appears at a significant level and dominant house-of-cards-like morphologies were observed only in the samples by $BC_{Ph\text{-}6\text{-}6\text{-}6}$ and $BC_{Ph\text{-}8\text{-}6\text{-}6}$. This result suggests that only proper chain lengths are favourable for the formation of house-of-cards-like morphologies.

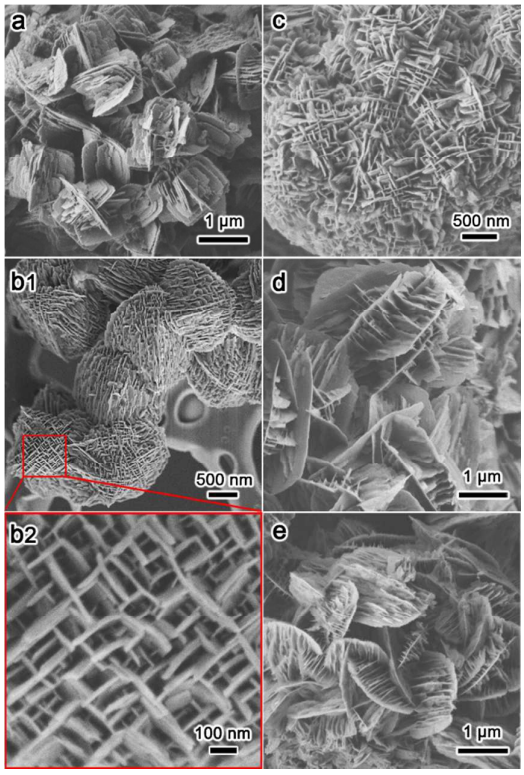

Fig. 8 SEM images of as-made samples synthesized by $BC_{Ph\text{-}4\text{-}6\text{-}6}$ (a), $BC_{Ph\text{-}6\text{-}6\text{-}6}$ (b1, b2), $BC_{Ph\text{-}8\text{-}6\text{-}6}$ (c), $BC_{Ph\text{-}10\text{-}6\text{-}6}$ (d), and $BC_{Ph\text{-}12\text{-}6\text{-}6}$ (d). Reprinted with permission from ref. 80. Copyright 2014. Nature Publishing Group.

In order to analyse the internal boundary structure, the TEM images of thin sections of the as-made samples synthesized by $BC_{Ph\text{-}6\text{-}6\text{-}6}$ were observed (Fig. 9). The perpendicular crystal plates with a boundary relationship shared a common c axis, in which the (100) faces are overgrown on the (010) faces. A possible structural model of the boundary is that the connectivity at the joints could arise through the formation of a new set of Si-O-Si bonds, which would sustain the lamellar structure. After calcination, the majority of the boundary layers did not completely collapse to produce clear mesopores because of the framework connectivity (Figs. 9c and d). In addition, the apparent house-of-cards-like morphology makes this type of SCZN-2 to possess well-defined micro-meso-macroporous architecture. Due to the successive rotational intergrowth, abundant mesopores were reserved after calcination, and the Brunauer-Emmett-Teller (BET) surface and mesopore volumes of SCZN-2 by $BC_{Ph\text{-}6\text{-}6\text{-}6}$ could reach to 658 $m^2\ g^{-1}$ and 0.51 $cm^3\ g^{-1}$ (Fig. 10), respectively. Compared with the spontaneous growth of zeolitic nanosheets by small SDAs, our strategy and the obtained samples by bolaform amphiphilic molecules clearly showed the advantage in available control on uniform mesoscopic porosity and crystallographic correlation between two perpendicular crystals.

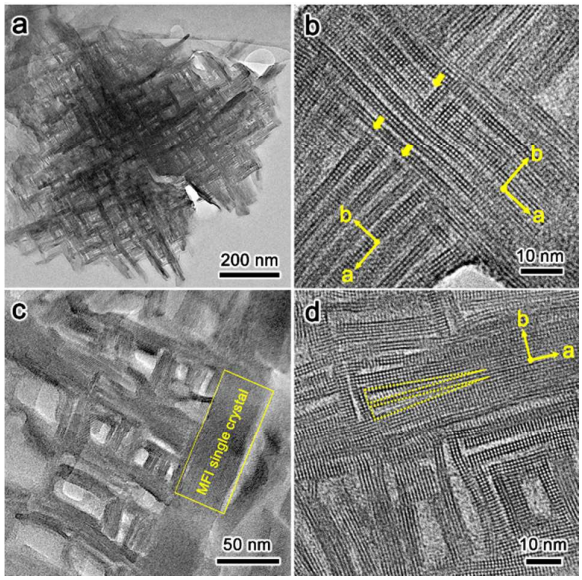

Fig. 9 HRTEM images of as-made (a, b) and calcined (c, d) SCZN-2 templated by $BC_{Ph\text{-}6\text{-}6\text{-}6}$. Reprinted with permission from ref. 80. Copyright 2014. Nature Publishing Group.

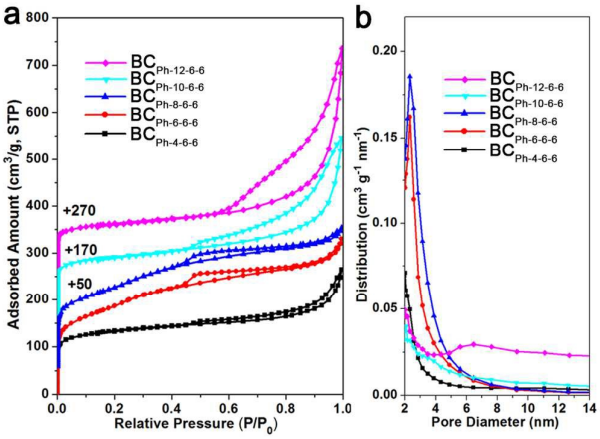

Fig. 10 The N_2 adsorption-desorption isotherms (**a**) and pore size distributions (**b**) of calcined SCZNs by $BC_{Ph\text{-}n\text{-}6\text{-}6}$. Reprinted with permission from ref. 80. Copyright 2014. Nature Publishing Group.

5. Synthesis of single-crystalline mesoporous ZSM-5 via triply branched cationic amphiphilic molecules.

As shown in sections 3 and 4, weather single branched $C_{Ph\text{-}Ph\text{-}10\text{-}6}$ or double branched $BC_{Ph\text{-}6\text{-}6\text{-}6}$ can only direct the formation of lamellar MFI nanosheets but cannot restrict the crystalline growth of zeolite along the *a*-*c* planes. Therefore, we designed a triply branched

cationic amphiphilic molecule. Compared to the double branched template, the third branch could also act as the SDA and further block the self-assembly of templates or crystalline growth of zeolite in the direction of *a*- or *c*- axis. Hierarchically porous zeolites with three-dimensional mesopores may be obtained owning to this novel strategy. As a consequence, we prepared a triply branched cationic amphiphilic molecule with the molecular configuration of Ph-(O-$C_{10}H_{20}$-$N^+(CH_3)_2$-C_6H_{12}-$N^+(CH_3)_2$-$C_6H_{13})_3$ ($6Br^-$) (denoted as $TC_{Ph\text{-}10\text{-}6\text{-}6}$). Single-crystalline mesoporous ZSM-5 (SCMZ) with three-dimensional mesopores was generated by using $TC_{Ph\text{-}10\text{-}6\text{-}6}$ as the sole SDA[81].

Figure 10a-c show the HRTEM images of a sliced thin section of the calcined SCMZ along the *a*-, *c*-, and *b*-axis, respectively. Abundant sheet-like mesopores with a thickness of ~2 nm were clearly observed. The selected-area electron diffraction (SAED) patterns corresponding to these HRTEM images indicate the formation of single-crystalline structure. The sheet-like mesopores embedded in the zeolitic framework did not collapse after calcination under high temperature, quite different from the samples synthesized by $C_{Ph\text{-}Ph\text{-}10\text{-}6}$ and $BC_{Ph\text{-}6\text{-}6\text{-}6}$. Owning to the formation of abundant mesopores, the calcined SCMZ possesses high BET surface area and mesopore volumes (496 $m^2 g^{-1}$ and 0.22 $cm^3 g^{-1}$, respectively), much larger than the ones of the conventional bulk ZSM-5[104, 105]. The sharp peak at ~2.1 nm in the pore size distribution (Fig. 10d) was approximately equal to the sheet thickness from the TEM observation.

The formation mechanism of SCMZ depends on the effective arrangements of the triply branched templates along the *a*-, *b*-, and *c*-axis of the MFI framework. Two of the three branched chains were aligned with the straight channels, and the third one directed the micropores along the zigzag channel. It's worth noting that not all of the branched chains could direct the formation of micropores but rather contributed to stabilize the zeolitic structure.

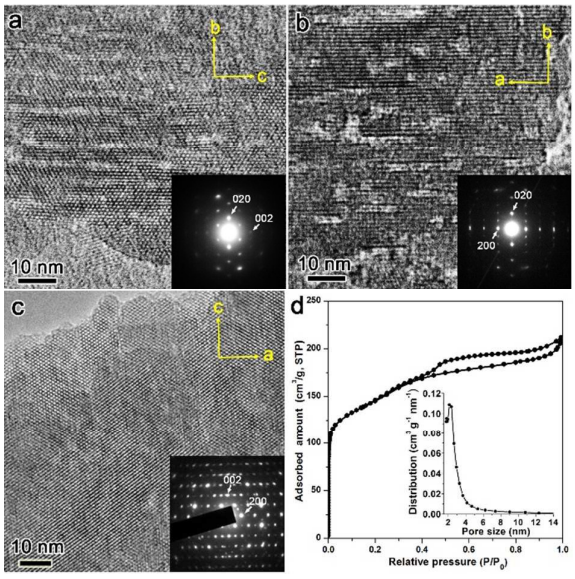

Fig. 11 TEM images (a-c) and their corresponding SAED patterns (insets), N_2 adsorption-desorption isotherm and pore size distribution (d) of the calcined SCMZ. Reprinted with permission from ref. 81. Copyright 2014. American Chemical Society.

6. Conclusion and Perspective

Hierarchically porous zeolites always attract enough attention especially in the petroleum chemical industry field. Although abundant attempts and strategies have been focused on the construction of the porous system, the synthesis of highly ordered porous zeolite is still a challenge unresolved. The strategy based on the self-assembly of novel amphiphilic molecules is supposed to be the most effective way. The surfactants with multi-quaternary ammonium head groups have successfully directed the formation of ordered MFI nanosheets and crystalline hexagonally-ordered mesoporous material without the additional small SDAs. As is well known, the interactions between the hydrophobic chains also play an important role in the molecular self-assembly[14, 106, 107]. Therefore, the design of the configuration of hydrophobic section may result in different self-assembling behavior and further realize the generation of ordered meso-structure in zeolites.

In this review, we present a design concept for the preparation of novel amphiphilic molecules which then can act as the sole templates to build hierarchically porous zeolites. Based on the thorough study of structrural-directing mechanism of CTAB in the synthesis of ZSM-5, aromatic groups are introduced into the hydrophobic chains. Owning to the π-π stacking, templates with single quaternary ammonium head group are equipped with the power to synthesize ordered MFI nanosheets. Furthermore, based on the results of molecular mechanics calculations, bolaform amphiphilic molecules are designed to construct the 90° rotational intergrowth structures on the basis of single-crystalline MFI nanosheets. Due to the connectivity of zeolitic framework, abundant mesopores are preserved after calcination. Finally, Single-crystalline mesoporous ZSM-5 can be obtained by using the triply branched cationic surfactant. Via the design of different molecular configuration, we achieve the construction of hierarchical mesopores in zeolitic frameworks from two-dimensional to three-dimensional.

Our strategies for the synthesis of porous zeolites provide an important reference to govern the organic molecular self-assembly and the crystalline growth of zeolites simultaneously. Following this design concept, more different kinds of intermolecular forces can be employed and various quaternary ammonium head groups can be changed in order to direct the distinct zeolitic frameworks (not just the MFI type). Furthermore, how to balance the coexistence of crystalline growth between ordered mesopores and micropores should be considered deeply when designing certain amphiphilic templates. The design concept of novel amphiphilic molecules used in the synthesis system of hierarchically porous system can be expanded to prepare other inorganic porous materials, in addition to siliceous species.

Acknowledgements

This work was supported by the National Basic Research Program (2013CB934101) and the National Natural Science Foundation (Grant No. 21471099) of China.

References

1. A. Corma, *Chem. Rev.*, 1997, **97**, 2373-2420.
2. M. E. Davis, *Nature*, 2002, **417**, 813-821.
3. A. Primo and H. Garcia, *Chem. Soc. Rev.*, 2014, **43**, 7548-7561.
4. A. Corma, S. Iborra and A. Velty, *Chem. Rev.*, 2007, **107**, 2411-2502.
5. I. Hill, A. Malek and A. Bhan, *ACS Catal.*, 2013, 1992-2001.
6. J. Kärger and D. Ruthven, *Diffusion in zeolites, Wiley, New York*, 1992.
7. N. Chen, T. Degnan and C. M. Smith, *Molecular transport and reaction in zeolites, VCH, New York*, 1994.
8. Y. Tao, H. Kanoh, L. Abrams and K. Kaneko, *Chem. Rev*, 2006, **106**, 896-910.
9. K. P. de Jong, J. Zečević and H. Friedrich, *Angew. Chem.*, 2010, **122**, 10272-10276.
10. D. E. Akporiaye, *Angew. Chem. Int. Ed.*, 1998, **37**, 2456-2457.
11. K. Möller and T. Bein, *Chem. Soc. Rev.*, 2013, **42**, 3689-3707.
12. C. T. Kresge, M. E. Leonowicz, W. J. Roth, J. C. Vartuli and J. S. Beck, *Nature*, 1992, **359**, 710-712.
13. A. Monnier, F. Schüth, Q. Huo, D. Kumar, D. Margolese, R. S. Maxwell, G. D. Stucky, M. Krishnamurty, P. Petroff, A. Firouzi, M. Janicke and B. F. Chmelka, *Science*, 1993, **261**, 1299-1303.
14. Y. Wan and Zhao, *Chem. Rev.*, 2007, **107**, 2821-2860.
15. V. Meynen, P. Cool and E. F. Vansant, *Microporous Mesoporous Mater.*, 2009, **125**, 170-223.
16. K. Egeblad, C. H. Christensen, M. Kustova and C. H. Christensen, *Chem. Mater.*, 2008, **20**, 946-960.
17. S. Lopez-Orozco, A. Inayat, A. Schwab, T. Selvam and W. Schwieger, *Adv. Mater.*, 2011, **23**, 2602-2615.
18. C. Perego and R. Millini, *Chem. Soc. Rev.*, 2013, **42**, 3956-3976.
19. D. P. Serrano, J. M. Escola and P. Pizarro, *Chem. Soc. Rev.*, 2013, **42**, 4004-4035.
20. M. E. Davis, *Chem. Mater.*, 2014, **26**, 239-245.
21. S. Mitchell, A. B. Pinar, J. Kenvin, P. Crivelli, J. Kärger and J. Pérez-Ramírez, *Nat. commun.*, 2015, **6**, 8633, doi:8610.1038/ncomms9633.
22. M. Moliner, *Top. Catal.*, 2015, **58**, 502-512.
23. L. Tosheva and V. P. Valtchev, *Chem. Mater.*, 2005, **17**, 2494-2513.
24. K. Möller, B. Yilmaz, R. M. Jacubinas, U. Müller and T. Bein, *J. Am. Chem. Soc.*, 2011, **133**, 5284-5295.
25. A. Corma, V. Fornes, S. B. Pergher, T. L. M. Maesen and J. G. Buglass, *Nature*, 1998, **396**, 353-356.
26. Y. Liu, W. Zhang and T. J. Pinnavaia, *J. Am. Chem. Soc.*, 2000, **122**, 8791-8792.
27. Y. Liu, W. Zhang and T. J. Pinnavaia, *Angew. Chem. Int. Ed.*, 2001, **40**, 1255-1258.
28. W. Chaikittisilp, Y. Suzuki, R. R. Mukti, T. Suzuki, K. Sugita, K. Itabashi, A. Shimojima and T. Okubo, *Angew. Chem. Int. Ed.*, 2013, **125**, 3439-3443.
29. X. Zhang, D. Liu, D. Xu, S. Asahina, K. A. Cychosz, K. V. Agrawal, Y. Al Wahedi, A. Bhan, S. Al Hashimi, O. Terasaki, M. Thommes and M. Tsapatsis, *Science*, 2012, **336**, 1684-1687.
30. D. Xu, G. R. Swindlehurst, H. Wu, D. H. Olson, X. Zhang and M. Tsapatsis, *Adv. Funct. Mater.*, 2013, **24**, 201-208.
31. S. van Donk, A. H. Janssen, J. H. Bitter and K. P. de Jong, *Catal. Rev.*, 2003, **45**, 297-319.
32. H. G. Karge, P. Anderson and J. Weitkamp, *Post-Synthesis Modification I*, Springer, 2002.
33. A. H. Janssen, A. J. Koster and K. P. de Jong, *Angew. Chem. Int. Ed.*, 2001, **40**, 1102-1104.
34. D. Verboekend and J. Pérez-Ramírez, *Catal. Sci. Technol.*, 2011, **1**, 879-890.
35. J. C. Groen, J. A. Moulijn and J. Pérez-Ramírez, *J. Mater. Chem.*, 2006, **16**, 2121-2131.
36. J. Pérez‐Ramírez, S. Abello, A. Bonilla and J. C. Groen, *Adv. Funct. Mater.*, 2009, **19**, 164-172.
37. C. J. H. Jacobsen, C. Madsen, J. Houzvicka, I. Schmidt and A. Carlsson, *J. Am. Chem. Soc.*, 2000, **122**, 7116-7117.
38. A. Janssen, I. Schmidt, C. Jacobsen, A. Koster and K. De Jong, *Microporous Mesoporous Mater.*, 2003, **65**, 59-75.
39. I. Schmidt, A. Boisen, E. Gustavsson, K. Ståhl, S. Pehrson, S. Dahl, A. Carlsson and C. J. Jacobsen, *Chem. Mater.*, 2001, **13**, 4416-4418.
40. Y. Tao, H. Kanoh and K. Kaneko, *J. Am. Chem. Soc.*, 2003, **125**, 6044-6045.
41. A. Sakthivel, S.-J. Huang, W.-H. Chen, Z.-H. Lan, K.-H. Chen, T.-W. Kim, R. Ryoo, A. S. T. Chiang and S.-B. Liu, *Chem. Mater.*, 2004, **16**, 3168-3175.
42. Z. Yang, Y. Xia and R. Mokaya, *Adv. Mater.*, 2004, **16**, 727-732.
43. B. Li, Z. Hu, B. Kong, J. Wang, W. Li, Z. Sun, X. Qian, Y. Yang, W. Shen, H. Xu and D. Zhao, *Chem. Sci.*, 2014, **5**, 1565-1573.
44. H. Zhu, Z. Liu, Y. Wang, D. Kong, X. Yuan and Z. Xie, *Chem. Mater.*, 2008, **20**, 1134-1139.
45. W. Fan, M. A. Snyder, S. Kumar, P.-S. Lee, W. C. Yoo, A. V. McCormick, R. Lee Penn, A. Stein and M. Tsapatsis, *Nat. Mater.*, 2008, **7**, 984-991.
46. H. Chen, J. Wydra, X. Zhang, P.-S. Lee, Z. Wang, W. Fan and M. Tsapatsis, *J. Am. Chem. Soc.*, 2011, **133**, 12390-12393.
47. F. N. Gu, F. Wei, J. Y. Yang, N. Lin, W. G. Lin, Y. Wang and J. H. Zhu, *Chem. Mater.*, 2010, **22**, 2442-2450.
48. Y. Zhu, Z. Hua, J. Zhou, L. Wang, J. Zhao, Y. Gong, W. Wu, M. Ruan and J. Shi, *Chem. Eur. J.*, 2011, **17**, 14618-14627.
49. W. Guo, C. Xiong, L. Huang and Q. Li, *J. Mater. Chem.*, 2001, **11**, 1886-1890.
50. A. Kulak, Y.-J. Lee, Y. S. Park, H. S. Kim, G. S. Lee and K. B. Yoon, *Adv. Mater.*, 2002, **14**, 526.
51. Z. Wang, L. Xu, J.-g. Jiang, Y. Liu, M. He and P. Wu, *Microporous Mesoporous Mater.*, 2012, **156**, 106-114.
52. M. Choi, H. S. Cho, R. Srivastava, C. Venkatesan, D.-H. Choi and R. Ryoo, *Nat. Mater.*, 2006, **5**, 718-723.
53. K. Cho, R. Ryoo, S. Asahina, C. Xiao, M. Klingstedt, A. Umemura, M. W. Anderson and O. Terasaki, *Solid State Sci.*, 2011, **13**, 750-756.
54. D.-H. Lee, M. Choi, B.-W. Yu and R. Ryoo, *Chem. Commun.*, 2009, 74-76.
55. M. Choi, R. Srivastava and R. Ryoo, *Chem. Commun.*, 2006, 4380-4382.
56. H. Wang and T. J. Pinnavaia, *Angew. Chem. Int. Ed.*, 2006, **45**, 7603-7606.
57. A. Inayat, I. Knoke, E. Spiecker and W. Schwieger, *Angew. Chem. Int. Ed.*, 2012, **51**, 1962-1965.
58. L. Wang, Z. Zhang, C. Yin, Z. Shan and F.-S. Xiao, *Microporous Mesoporous Mater.*, 2010, **131**, 58-67.
59. S. Liu, X. Cao, L. Li, C. Li, Y. Ji and F.-S. Xiao, *Colloid Surf. A-Physicochem. Eng. Asp.*, 2008, **318**, 269-274.
60. F.-S. Xiao, L. Wang, C. Yin, K. Lin, Y. Di, J. Li, R. Xu, D. S. Su, R. Schlögl, T. Yokoi and T. Tatsumi, *Angew. Chem. Int. Ed.*, 2006, **45**, 3090-3093.
61. J. Zhu, Y. Zhu, L. Zhu, M. Rigutto, A. van der Made, C. Yang, S. Pan, L. Wang, L. Zhu, Y. Jin, Q. Sun, Q. Wu, X. Meng, D. Zhang, Y. Han, J. Li, Y. Chu, A. Zheng, S. Qiu, X. Zheng and F. S. Xiao, *J. Am. Chem. Soc.*, 2014, **136**, 2503-2510.

62. F. Liu, T. Willhammar, L. Wang, L. Zhu, Q. Sun, X. Meng, W. Carrillo-Cabrera, X. Zou and F.-S. Xiao, *J. Am. Chem. Soc.*, 2012, **134**, 4557-4560.
63. K. Na, M. Choi and R. Ryoo, *Microporous Mesoporous Mater.*, 2013, **166**, 3-19.
64. K. Na, M. Choi, W. Park, Y. Sakamoto, O. Terasaki and R. Ryoo, *J. Am. Chem. Soc.*, 2010, **132**, 4169-4177.
65. M. Choi, K. Na, J. Kim, Y. Sakamoto, O. Terasaki and R. Ryoo, *Nature*, 2009, **461**, 246-249.
66. K. Na, C. Jo, J. Kim, W.-S. Ahn and R. Ryoo, *ACS Catal.*, 2011, **1**, 901-907.
67. K. Na, W. Park, Y. Seo and R. Ryoo, *Chem. Mater.*, 2011, **23**, 1273-1279.
68. W. Park, D. Yu, K. Na, K. E. Jelfs, B. Slater, Y. Sakamoto and R. Ryoo, *Chem. Mater.*, 2011, **23**, 5131-5137.
69. J. Jung, C. Jo, K. Cho and R. Ryoo, *J. Mater. Chem.*, 2012, **22**, 4637.
70. C. Jo, R. Ryoo, N. Žilková, D. Vitvarová and J. Čejka, *Catal. Sci. Technol.*, 2013, **3**, 2119.
71. R. J. Messinger, K. Na, Y. Seo, R. Ryoo and B. F. Chmelka, *Angew. Chem. Int. Ed.*, 2015, **54**, 927-931.
72. K. Na, C. Jo, J. Kim, K. Cho, J. Jung, Y. Seo, R. J. Messinger, B. F. Chmelka and R. Ryoo, *Science*, 2011, **333**, 328-332.
73. K. Cho, K. Na, J. Kim, O. Terasaki and R. Ryoo, *Chem. Mater.*, 2012, **24**, 2733-2738.
74. C. Jo, Y. Seo, K. Cho, J. Kim, H. S. Shin, M. Lee, J. C. Kim, S. O. Kim, J. Y. Lee and H. Ihee, *Angew. Chem.*, 2014, **126**, 5217-5221.
75. C. Jo, J. Jung, H. S. Shin, J. Kim and R. Ryoo, *Angew. Chem.*, 2013, **125**, 10198-10201.
76. Z. Wang, J. Yu and R. Xu, *Chem. Soc. Rev.*, 2012, **41**, 1729-1741.
77. K. Li, J. Valla and J. Garcia-Martinez, *ChemCatChem*, 2014, **6**, 46-66.
78. D. Xu, J. Feng and S. Che, *Dalton Trans.*, 2014, **43**, 3612-3617.
79. D. Xu, Z. Jing, F. Cao, H. Sun and S. Che, *Chem. Mater.*, 2014, **26**, 4612-4619.
80. D. Xu, Y. Ma, Z. Jing, L. Han, B. Singh, J. Feng, X. Shen, F. Cao, P. Oleynikov, H. Sun, O. Terasaki and S. Che, *Nat. Commun.*, 2014, **5**, DOI: 10.1038/ncomms5262.
81. B. K. Singh, D. Xu, L. Han, J. Ding, Y. Wang and S. Che, *Chem. Mater.*, 2014, **26**, 7183-7188.
82. M. E. Davis and R. F. Lobo, *Chem. Mater.*, 1992, **4**, 756-768.
83. C. S. Cundy and P. A. Cox, *Microporous Mesoporous Mater.*, 2005, **82**, 1-78.
84. Y. Kubota, M. M. Helmkamp, S. I. Zones and M. E. Davis, *Microporous Mater.*, 1996, **6**, 213-229.
85. J. C. Jansen, in *Stud. Surf. Sci. Catal.*, eds. E. M. F. P. A. J. H. van Bekkum and J. C. Jansen, Elsevier, 2001, vol. Volume 137, pp. 175-227.
86. C. E. Kirschhock, R. Ravishankar, P. Jacobs and J. Martens, *J. Phys. Chem. B*, 1999, **103**, 11021-11027.
87. S. L. Burkett and M. E. Davis, *Chem. Mater.*, 1995, **7**, 920-928.
88. X. Chen, L. Huang and Q. Li, *J. Phys. Chem. B*, 1997, **101**, 8460-8467.
89. J. S. Beck, J. C. Vartuli, G. J. Kennedy, C. T. Kresge, W. J. Roth and S. E. Schramm, *Chem. Mater.*, 1994, **6**, 1816-1821.
90. L. Huang, X. Chen and Q. Li, *J. Mater. Chem.*, 2001, **11**, 610-615.
91. T. Moteki, S. H. Keoh and T. Okubo, *Chem. Commun.*, 2014, **50**, 1330-1333.
92. C. A. Hunter, K. R. Lawson, J. Perkins and C. J. Urch, *J. Chem. Soc., Perkin Trans. 2*, 2001, **0**, 651-669.
93. T. Kunitake, Y. Okahata, M. Shimomura, S. Yasunami and K. Takarabe, *J. Am. Chem. Soc.*, 1981, **103**, 5401-5413.
94. C. A. Hunter and J. K. Sanders, *J. Am. Chem. Soc.*, 1990, **112**, 5525-5534.
95. M. Lee, B.-K. Cho, H. Kim, J.-Y. Yoon and W.-C. Zin, *J. Am. Chem. Soc.*, 1998, **120**, 9168-9179.
96. M. O. Sinnokrot and C. D. Sherrill, *J. Am. Chem. Soc.*, 2004, **126**, 7690-7697.
97. D. Zhang, P. Oleynikov, S. Hovmöller and X. Zou, *Zeitschrift für Kristallographie International journal for structural, physical, and chemical aspects of crystalline materials*, 2010, **225**, 94-102.
98. S. J. Marrink, A. H. de Vries and A. E. Mark, *J. Phys. Chem. B*, 2004, **108**, 750-760.
99. D. C. Liu and J. Nocedal, *Math. Program.*, 1989, **45**, 503-528.
100. L. Karwacki, E. Stavitski, M. H. Kox, J. Kornatowski and B. M. Weckhuysen, *Angew. Chem.*, 2007, **119**, 7366-7369.
101. W. Chaikittisilp, M. E. Davis and T. Okubo, *Chem. Mater.*, 2007, **19**, 4120-4122.
102. W.-g. Kim, X. Zhang, J. S. Lee, M. Tsapatsis and S. Nair, *ACS nano*, 2012, **6**, 9978-9988.
103. E. Stavitski, M. R. Drury, D. A. M. de Winter, M. H. F. Kox and B. M. Weckhuysen, *Angew. Chem. Int. Ed.*, 2008, **47**, 5637-5640.
104. P. Wang, B. Shen and J. Gao, *Catal. Today*, 2007, **125**, 155-162.
105. S. Sang, F. Chang, Z. Liu, C. He, Y. He and L. Xu, *Catal. Today*, 2004, **93-95**, 729-734.
106. Q. Huo, D. I. Margolese and G. D. Stucky, *Chem. Mater.*, 1996, **8**, 1147-1160.
107. G. D. Stucky, Q. Huo, A. Firouzi, B. F. Chmelka, S. Schacht, I. Voigt-Martin and F. Schüth, *Stud. Surf. Sci. Catal.*, 1997, **105**, 3-28.

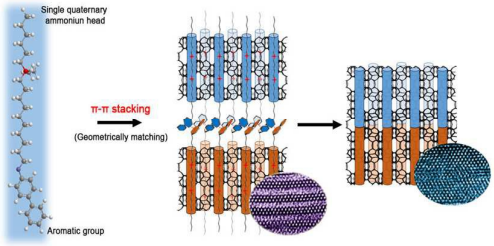

The π-π stacking of aromatic groups and a geometrical matching between their arrangement and the zeolitic framework leading to the single-crystalline zeolite mesostructures.